International Journal of Rock Mechanics & Mining Sciences ■ (■■■■) ■■■–■■■

Contents lists available at ScienceDirect

International Journal of Rock Mechanics & Mining Sciences

journal homepage: www.elsevier.com/locate/ijrmms

A novel and versatile apparatus for brittle rock deformation

Cristiano Collettini [a,b,*], Giuseppe Di Stefano [b], Brett Carpenter [b], Piergiorgio Scarlato [b], Telemaco Tesei [b,c], Silvio Mollo [b], Fabio Trippetta [a], Chris Marone [d], Gianni Romeo [b], Lauro Chiaraluce [b]

[a] Dipartimento di Scienze della Terra, Università degli Studi La Sapienza, Rome, Italy
[b] Istituto Nazionale di Geofisica e Vulcanologia, Rome, Italy
[c] Dipartimento di Scienze della Terra, Università degli Studi di Perugia, Perugia, Italy
[d] Rock and Sediment Mechanics Laboratory, Penn State University, USA

ARTICLE INFO

Article history:
Received 8 May 2013
Received in revised form
3 November 2013
Accepted 24 December 2013

Keywords:
Biaxial apparatus
Pressure vessel
Friction

ABSTRACT

This paper describes a new biaxial rock deformation apparatus within a pressure vessel, consisting of a stainless steel vessel with an internal diameter of 40 cm and six main access ports for electronics (~100 pins), pore fluids (three lines), and confining oil. The apparatus has to ability to work on large rock samples, up to 20 × 20 cm^2, with horizontal and vertical forces up to 1.5 MN. The maximum confining pressure of the vessel is 70 MPa, and fluid flow properties and permeability of large-samples can be tested using up to 8 L of fluids that can be pressurized up to 30 MPa. Sliding velocity during experiments is in the range 0.1 μm/s – 1.0 cm/s. The machine stiffness is 0.91 kN/μm and 1.3 kN/μm for the vertical and horizontal axes, respectively. Measurements on friction, velocity dependence of friction and healing properties of reference material like granite and talc replicate the values presented in the literature. Triaxial stress state tests with controlled confining and pore fluid pressure, and fluid flow through the samples have been performed successfully. The machine is extremely versatile, as it works as a uniaxial, triaxial or true-triaxial apparatus, on rock samples with dimensions ranging from several to tens of centimetres. Due to the broad number of potential operating conditions, we decided to name the machine BRAVA: Brittle Rock deformAtion Versatile Apparatus.

1. Introduction

A typical biaxial apparatus consists of vertical and horizontal load frames that are used to apply normal and shear forces on a fault rock sample. In the double-direct shear configuration [1–3], three rigid forcing blocks, one center block and two side blocks, sandwich two identical layers of the fault rock (Fig. 1). The horizontal piston applies a constant horizontal force, holding the blocks in place. The center block is then forced between the two stationary side blocks by applying either a constant sliding velocity or constant vertical force through the vertical piston.

The biaxial deformation apparatus is an important piece of equipment used to study the frictional properties of fault rocks. Different designs, each with their own strengths, have been constructed in various rock deformation laboratories around the world. One of the first biaxial apparatus used to investigate the frictional properties of rocks was built at USGS in Menlo Park, USA [1]. Subsequently, a large biaxial press was then developed in the same USGS laboratory. This press is capable of working on samples 150 cm × 150 cm × 40 cm with a precut fault surface (200 cm long) along the diagonal [4]. In this apparatus, the increased specimen size provides opportunities for improved recording resolution and greater control of experimental variables [4,5]. Another pioneer apparatus, used to investigate rock friction and its implications for earthquake mechanisms, was built at the Lamont–Doherty Earth Observatory, USA [6]. In this apparatus, the rock sample is a slab, 3 cm × 3 cm × 18 cm, with a saw cut inclined at 30° across its major faces. The assembly is loaded in a biaxial loading frame fitted with two 1 MN hydraulic pistons. A high temperature biaxial frictional testing apparatus is hosted at Kyoto University [7]. The machine can exert a force of ~200 kN on fault rock samples with dimensions of several centimeters. The sample assembly is covered by a furnace that controls temperature up to 1000 °C. At Tokyo University, a large double-shear loading apparatus was constructed [2]. In this apparatus, the length and thickness of rock samples are 100 cm and 10 cm respectively. Axial forces up to 3 MN are possible and horizontal force is exerted by three independent jacks (100 kN each), which can apply both uniform and non-uniform forces. A large biaxial apparatus is housed at the

* Corresponding author at: Dipartimento di Scienze della Terra, Università degli Studi La Sapienza, Rome, Italy. Tel.: +39 649914559; fax: +39 64454729.
E-mail address: cristiano.collettini@uniroma1.it (C. Collettini).

1365-1609/$ - see front matter © 2014 Elsevier Ltd. All rights reserved.
http://dx.doi.org/10.1016/j.ijrmms.2013.12.005

Institute of Geology in Beijing, China. This machine can work with fault rock samples with dimensions of 50 cm × 50 cm and thicknesses up to 30 cm [8]. A biaxial apparatus that has significantly contributed to our improved understanding on the frictional properties of fault rocks and sliding surfaces (more than 50 papers based on data collected from this machine have been published in the last decade) is found in the Rock and Sediment Mechanics Laboratory at the Pennsylvania State University (PSU). This machine can work with a maximum force of 1 MN on rock samples with dimensions up to 20×20 cm^2. Each load frame may be operated in displacement or load feedback servo control; displacement resolution is 0.1 μm and load resolution is 0.1 kN [9–12].

Although biaxial machines are key-apparatus to study the frictional properties of sliding surfaces and fault gouge, some important parameters for fault mechanics, such as fluid pressure and confining pressure, cannot be tested in the simple biaxial configuration. For this reason, the laboratory at PSU designed a pressure vessel that is positioned within the horizontal and vertical load frames [13,14].

In this manuscript, we present a new biaxial deformation apparatus integrated within a pressure vessel. This new apparatus is based on the system at PSU [15–17]. In order to work on larger rock samples, we designed a large vessel that would act as a combined load frame and pressure vessel (Fig. 2a). The machine is suitable for testing the petro-physical properties and mechanical/hydrologic behaviour of brittle rocks and fault rocks. At the same time, it is extremely versatile since it can work in uniaxial, triaxial (Fig. 2b) and true-triaxial (Fig. 2c) configurations, in the sense that we have the control of three independent forces, and can be used to test rock samples with dimensions ranging from several to 20 cm. Due to this versatility, we have decided to name it BRAVA: Brittle Rock deformAtion Versatile Apparatus.

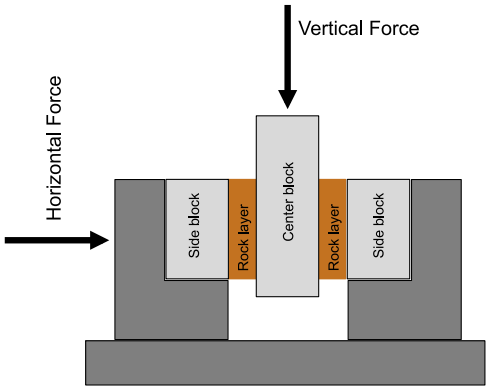

Fig. 1. Double direct shear geometry.

2. Design of the apparatus

The machine (Fig. 2a) is 2.5 m long, 2 m wide, 2.6 m high and weight 6000 kg. The apparatus consists of two orthogonal hydraulic pistons (P_V and P_H), three intensifier pistons (P_{PA}, P_{PB} and P_c), P, a pressure vessel (V), a panel with hydraulic components to drive the pistons (HC) and a box for the controlling system (CS). All parts of the apparatus are mounted on a cart. The hydraulic power supply is positioned on the roof of the laboratory, about 5 m away from the machine. The two main pistons are mounted on the vessel (Fig. 2a): one is mounted on vertical direction, P_V, for applying vertical load, the other is horizontal, P_H, for horizontal load on the experiment. The other three intensifiers are positioned on the cart (Fig. 2a): two control pore fluids P_{PA} and P_{PB} and the third one, confining oil, P_C.

In the standard triaxial configuration (Fig. 2b), the vertical load is applied by P_V, confining pressure is exerted by P_C whereas P_{PA} and P_{PB} can impose a constant pore fluid pressure or a pore pressure gradient to evaluate permeability of the rock sample. In the true-triaxial configuration (Fig. 2c), vertical and horizontal loads are applied by P_V and P_H, respectively. P_C controls the confining pressure and P_{PA} and P_{PB} can exert a constant pore fluid pressure or a constant fluid flux perpendicular to the rock layer. In the following, we will describe the different parts of the apparatus.

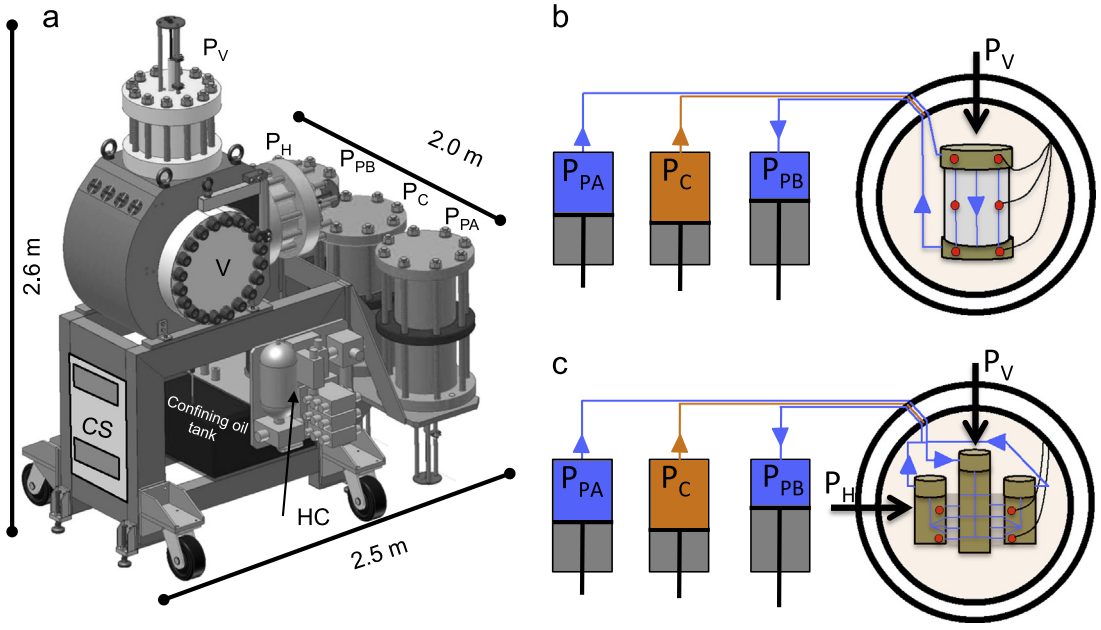

Fig. 2. (a) Schematic representation of BRAVA with the hydraulic pistons for vertical (P_V) and horizontal pressure (P_H), and the intensifiers for pore fluid pressure (P_{PA} and P_{PB}) and confining pressure (P_C), the vessel (V), the hydraulic control panel (HC) and the controlling system box (CS). (b) Standard triaxial configuration with pore fluid flow path. (c) True-triaxial configuration, with pore fluid flow path. In both configurations red circles are acoustic sensors. (For interpretation of the references to colour in this figure legend, the reader is referred to the web version of this article.)

Please cite this article as: Collettini C, et al. A novel and versatile apparatus for brittle rock deformation. Int J Rock Mech Mining Sci (2014), http://dx.doi.org/10.1016/j.ijrmms.2013.12.005

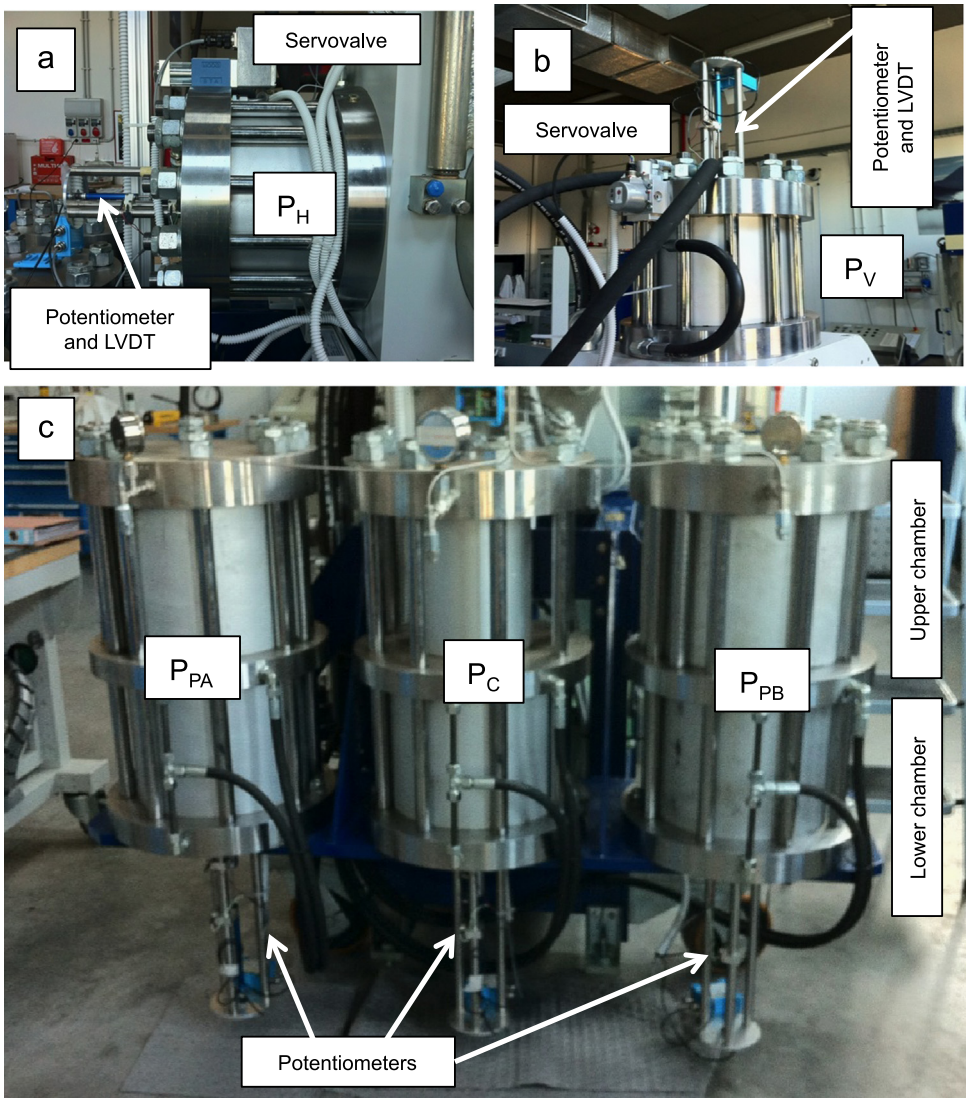

Fig. 3. Details of the intensifiers.

2.1. The five pistons

The five pistons were designed and built by Polytec, s.a.s., located in Padova, Italy. The vertical piston, P_V (Fig. 3), with a stroke of 100 mm, is fixed and sealed to the vessel and it is capable of exerting a force up to 1.5 MN. A MOOG 765 servovalve, mounted on the upper part of the cylinder, is used to allow high dynamic performances, i.e. accurate sliding velocity (0.1 μm/s–1.0 cm/s), fast response upon velocity changes, and stable forces. A potentiometer and LVDT are mounted on the upper side of the piston and read the displacement with a resolution of 0.1 μm. A load cell that is alignment and fixed at the end of the piston and measures the force over the range of 0.2–1000 kN and a resolution of 0.03 kN. The horizontal piston, P_H (Fig. 3), has all the characteristics of the vertical one, with the one difference being that the stroke is 50 mm.

The two intensifiers, P_{PA} and P_{PB}, are used for the fluid pressure and fluid flow through the sample (Fig. 3c). Given the internal configuration of the cylinder, 30 MPa is the maximum pore fluid pressure. One characteristic of these two intensifiers is their large dimensions (1000 mm high, 200 mm external diameter, 500 kg of weight, stroke 140 mm) that allow the use ~8 L of volume for fluid flow experiments. The intensifier for the confining oil, P_C, has dimensions similar to P_{PA} and P_{PB} (Fig. 3c) and it allows the generation of confining pressures up to 70 MPa.

Three potentiometers (Fig. 3c), similar to those used for P_V and P_H, are mounted at the bottom of P_{PA}, P_{PB} and P_C. Three Duplomatic DXJ3-DOL/5 servovalves, mounted on the hydraulic control panel (Fig. 5c), are used to operate P_{PA}, P_{PB} and P_c.

2.2. Pressure vessel

The stainless steel vessel (Fig. 4a and b), weight of 1650 kg, has an external diameter of 900 mm and an internal diameter of 400 mm. The vessel is designed to support the vertical and horizontal pistons. Two doors, 200 kg each, are equipped with 20 bolts (M32 size) that serve to close the vessel. To prevent confining oil leakage, O-rings are mounted on each door. The doors are suspended with an arm that allows easy rotation and translation. The vessel includes six high-pressure (up to 70 MPa) access ports that are used for electronics (~100 pins), pore fluids (3 lines) and confining oil (Fig. 4c). Another access port located at the bottom of the vessel is used to fill/empty the vessel with confining oil. The oil for confinement is 13,8660 VE 15–68 Vaselina Enologica (Green Star High Tech lubricants and additives) that is contained within a tank (80 L of capacity) located below the vessel (Fig. 2). An electric

Please cite this article as: Collettini C, et al. A novel and versatile apparatus for brittle rock deformation. Int J Rock Mech Mining Sci (2014), http://dx.doi.org/10.1016/j.ijrmms.2013.12.005

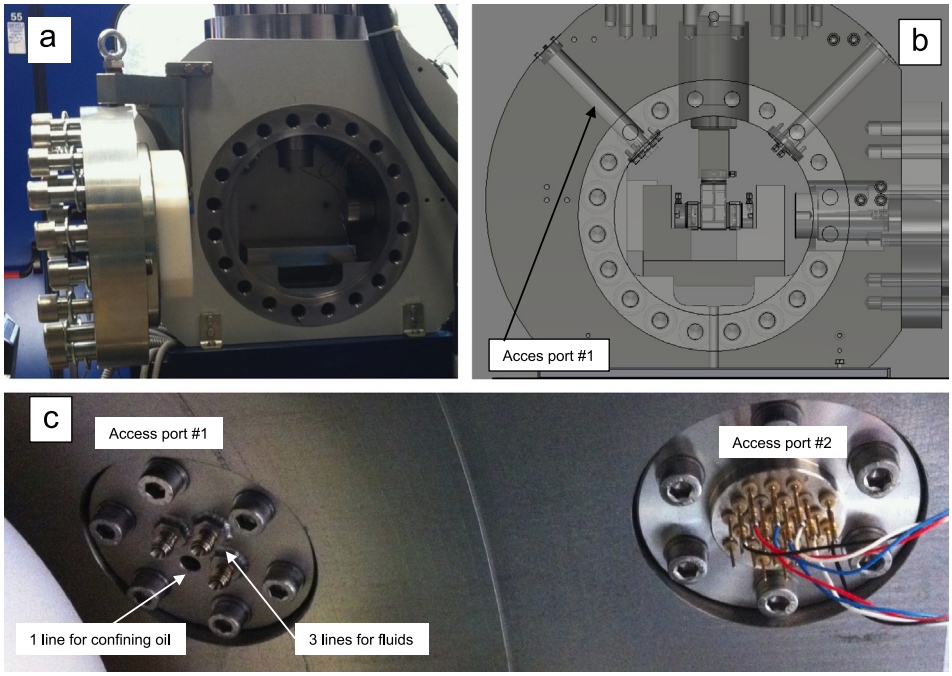

Fig. 4. (a) and (b) Pressure vessel. (c) Details of the high-pressure ports for pore fluids and confining oil (left side), and electronics (right side).

motor with a pump, located above the tank (Fig. 2), is used to fill the pressure vessel. The infill of the vessel requires 40–50 L of confining oil and this operation takes about 30 min.

2.3. The hydraulic power supply and oil-dynamic circuit

The hydraulic power supply (Fig. 5a) was also built by Polytec, s.a.s., and includes two motors to power the hydraulic pistons of the machine. Motor M1 supplies the vertical and horizontal pistons, whereas Motor M2 supplies the three intensifiers for fluid and confining pressure. M1 is an 18 kW electric motor connected to a pump with a variable flow rate up to 42 l/min. M2 is a 4 kW motor connected to a pump with a flow rate up to 10 L/min. The oil tank (150 L of capacity) is connected to a cooling system composed of a chiller and heat exchanger (Fig. 5b). The heat exchanger is a 4-pass, water-cooled unit connected in series with a smaller, air-cooled unit. The series of oil cooling units are used to maintain a hydraulic oil temperature of about 50 °C, which translates into a steady hydraulic pump temperature of 60 °C.

Two on/off system valves are located on the Hydraulic Control Panel (Fig. 5c): system valve 1 (sv1) enables oil pressure to the vertical and horizontal pistons, system valve 2 (sv2) enables oil pressure to the three intensifiers located on the cart. A pressure stabilizer of 4.5 L capacity, and capable of sustaining a pressure of 330 bar, is connected with sv1 and sv2. The three servovalves that control P_{PA}, P_{PB} and P_C, are positioned on the Hydraulic Control Panel along with an oil filter.

2.4. The machine control/acquisition system

Two real time, RT, computers operate the machine. The first computer, RT1, is positioned on the machine and the second, RT2, is in the controlling console. RT1 is a single-board Re-programming Input/Output system, RIO, which operates in real time. RT1 is integrated with a field programmable gate array (FPGA) device. The FPGA board controls the machine at high regulating speeds and updates the control parameters during experiments. The controlling process, developed in LabVIEW, is very flexible and regulates the input signals of the servo-valves in order to control load, sliding velocity, confining-oil pressure, pore fluid flow and pore fluid pressure following the reference values from a target profile, depending on the experimental conditions. Using the console, the user can check the status of the machine and give main commands during experiments.

The scientific data acquisition is operated by a second flexible PXI-PC, the host PC, which reads the signals from interchangeable sensors (displacements, loads, pressure transducers and others) and can record data at frequencies from 1 Hz to 10 kHz. The host PC uses a high quality Analogue to Digital Converter, ADC-board, with 16 channels at 24 bits, for acquiring experimental data on the samples.

2.5. Forcing blocks

In the double-direct shear configuration, our rigid forcing blocks are constructed from stainless steel, with side blocks of dimensions $50 \times 50 \times 25$ mm^3, and a center block of dimensions $100 \times 50 \times 50$ mm^3 (e.g. Fig. 1). A constant contact area of 50×50 mm^2 is maintained during the experiment. To measure the frictional properties of fault rock and not those of the forcing-blocks fault rock contact, the faces of the forcing blocks in contact with the fault rock are grooved. These grooves show a trapezoidal shape with 2 mm and 0.7 mm lower and upper base respectively and 1 mm of height. Four steel guide plates are fixed on each side of the assembly to reduce lateral extrusion of the fault rock.

To measure simultaneously the frictional properties of fault rocks and the fluid flow and acoustic properties, we have designed different forcing blocks (Fig. 6). Each forcing block of the double-direct shear configuration is fitted with a high-pressure fluid port: a pore fluid inlet port in the central block and a pore fluid outlet port on each side block. The central block (Fig. 6a), with dimensions of $50 \times 50 \times 119$ mm^3, contains passages for fluids and six fluid distribution ports (three on each side) similarly surrounded by distribution channels that allow homogenous fluid access to both sides. The side blocks (Fig. 6b and c), with dimensions of $50 \times 50 \times 46$ mm^3, contain passages for both pore fluids and

Please cite this article as: Collettini C, et al. A novel and versatile apparatus for brittle rock deformation. Int J Rock Mech Mining Sci (2014), http://dx.doi.org/10.1016/j.ijrmms.2013.12.005

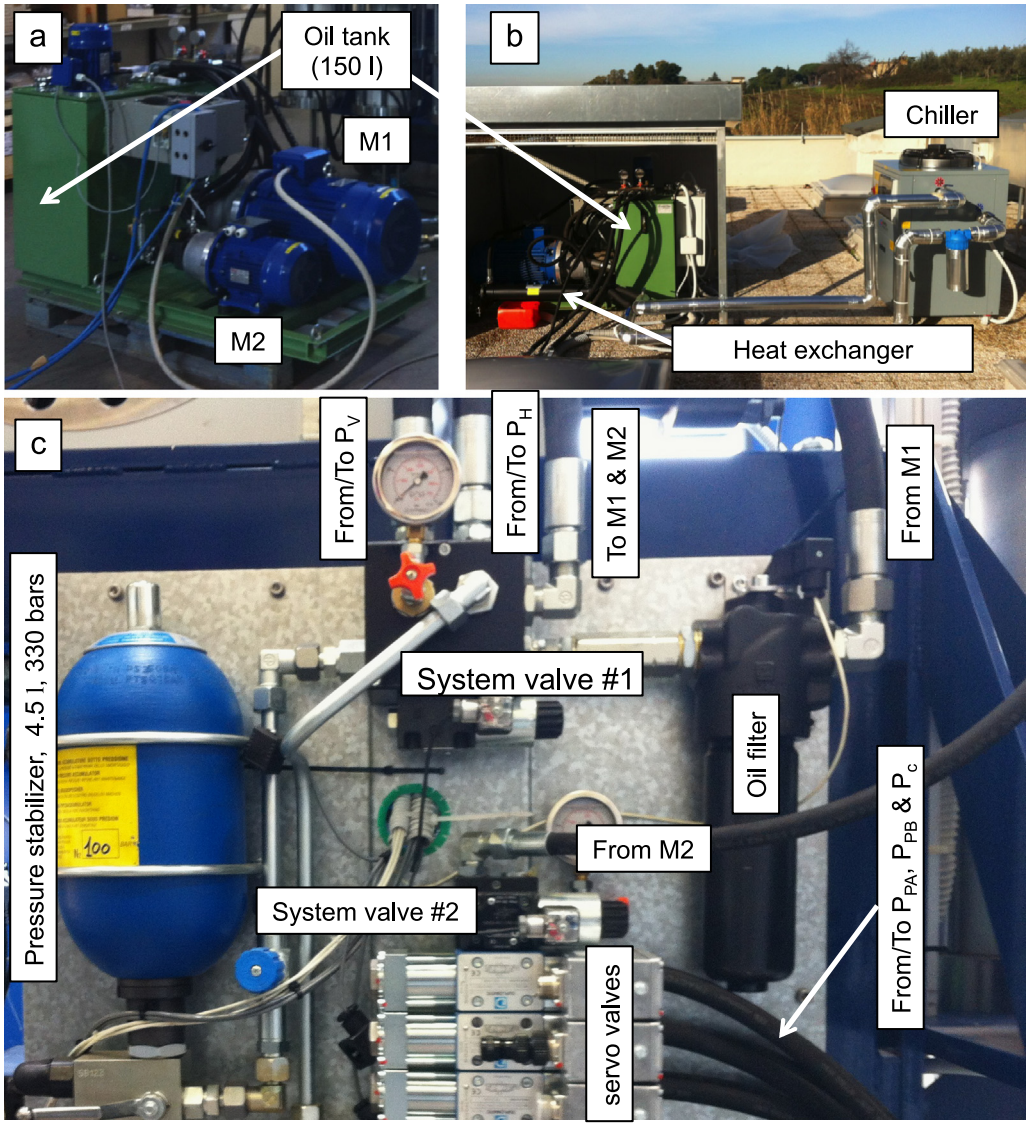

Fig. 5. (a) The hydraulic power supply with the two motors M1 and M2. (b) The hydraulic power supply linked to a heat exchanger and chiller for cooling the oil. (c) The hydraulic control panel (c.f. Fig. 2).

electronic connections to acoustic sensors. A double face platen (Fig. 6c) is fixed with four screws on each side block: the face positioned near the rock sample possesses distribution channels for pore fluids; the other face contains two cavities for the positioning of acoustic sensors. The channels for the electronic connections allow for potential contact between the acoustic sensors and confining oil. To prevent mixing between pore fluids and confining oil, two O-rings are located in the inner part of each side block (Fig. 6c). Fitted into each of the eight pore fluid distribution channels (six on the central block and two in the side blocks) are sintered, porous stainless steel frits, Mott Corporation, (Fig. 6d). The frits surfaces in contact with the fault rock are grooved to promote coupling at the layer boundary and shearing within the fault rock. Custom-made latex jackets (Fig. 6f) are used to cover the entire sample assembly and prevent mixing between the pore fluids and confining oil.

The forcing blocks allowing running experiments on rock samples of the dimension of 20×20 cm^2 (Fig. 7a and b) represent the most innovative and challenging aspects of the apparatus. These forcing blocks consist of a center block, a side block and a sensor block (Fig. 7a). Using these forcing blocks, the experiment will be conducted in a single direct shear configuration where a single rock layer, represented by powdered material or bare rock surfaces, is sandwiched between the center and the side block. With constant horizontal force applied, the center block is pushed downward by the vertical piston whereas the sensor block is in a stationary position (Fig. 7a). During the shearing of center block, the surface separating center and sensor blocks is greased in order to maintain friction close to zero. The side block has four cavities for installing acoustic sensors, two high-pressure fluid ports and a pipeline system for controlling pore fluid pressure (Fig. 7d). The inner part of the side block, the one into contact with the rock layer, has a higher and grooved zone with a cross shape (Fig. 7e). This grooved surface delimits four lower zones characterized by pore fluid distribution channels and a port for fluids (Fig. 7e). Four sintered, porous stainless steel frits are mounted above these lower zones forming a uniform grooved surface. The center block, with dimensions of 20×25 cm^2 (Fig. 7a and b), has two high-pressure fluid ports and a pipeline system for controlling pore fluid pressure (Fig. 7f); porous frits are mounted in a configuration similar to that of the side block. Since the center block is moving during the experiment, we decided to not insert acoustic sensors

Please cite this article as: Collettini C, et al. A novel and versatile apparatus for brittle rock deformation. Int J Rock Mech Mining Sci (2014), http://dx.doi.org/10.1016/j.ijrmms.2013.12.005

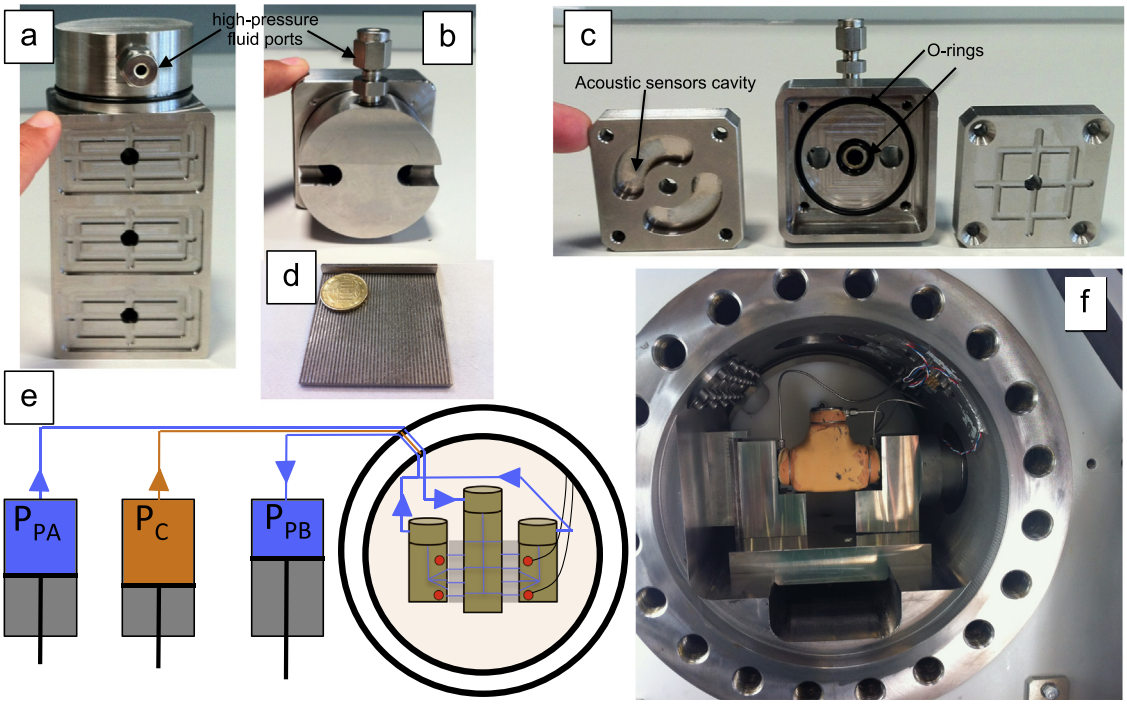

Fig. 6. Forcing blocks for measuring friction together with fluid flow and acoustic properties. (a) Center block. (b) Side block backside with the two holes for electronic cables. (c) Side block front side (central figure) and double face platen (side figures). (d) Grooved porous frits. (e) Experiment in true-triaxial configuration.

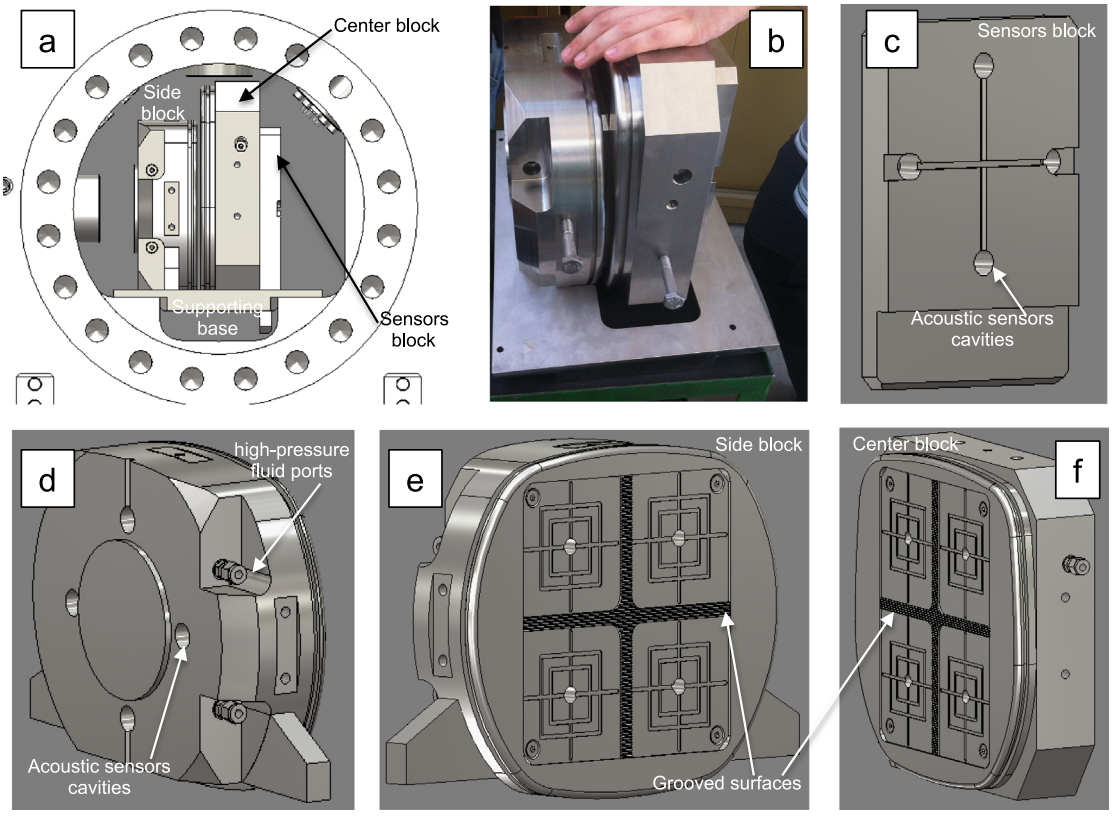

Fig. 7. Details of the 20×20 cm^2 forcing blocks.

in it. Acoustic sensors are positioned in the sensor block (Figs. 7a and c), which remains stationary during the experiment. The weight of the entire assemblage, including forcing blocks and the rock layer, is about 150 kg; consequently, sample construction and placement within the apparatus require the use of a small crane and pallet jack.

3. Tests of the machine

3.1. Machine stiffness

To determine the stiffness of the machine, we loaded stainless steel blocks with both the vertical and horizontal load pistons. The

Please cite this article as: Collettini C, et al. A novel and versatile apparatus for brittle rock deformation. Int J Rock Mech Mining Sci (2014), http://dx.doi.org/10.1016/j.ijrmms.2013.12.005

horizontal stiffness was determined by increasing the horizontal force by increments of 5 kN at low stresses and 50 kN at high stresses (Fig. 8a), and evaluating the associated shortening of the system (measured by the discussed LVDT). Each force increase is followed by a time interval (10–30 s) during which the force is maintained constant (Fig. 8b). After reaching 500 kN, we performed a step-down decrease in the horizontal force (Fig. 8a). The same procedure was adopted for the vertical load piston. In a

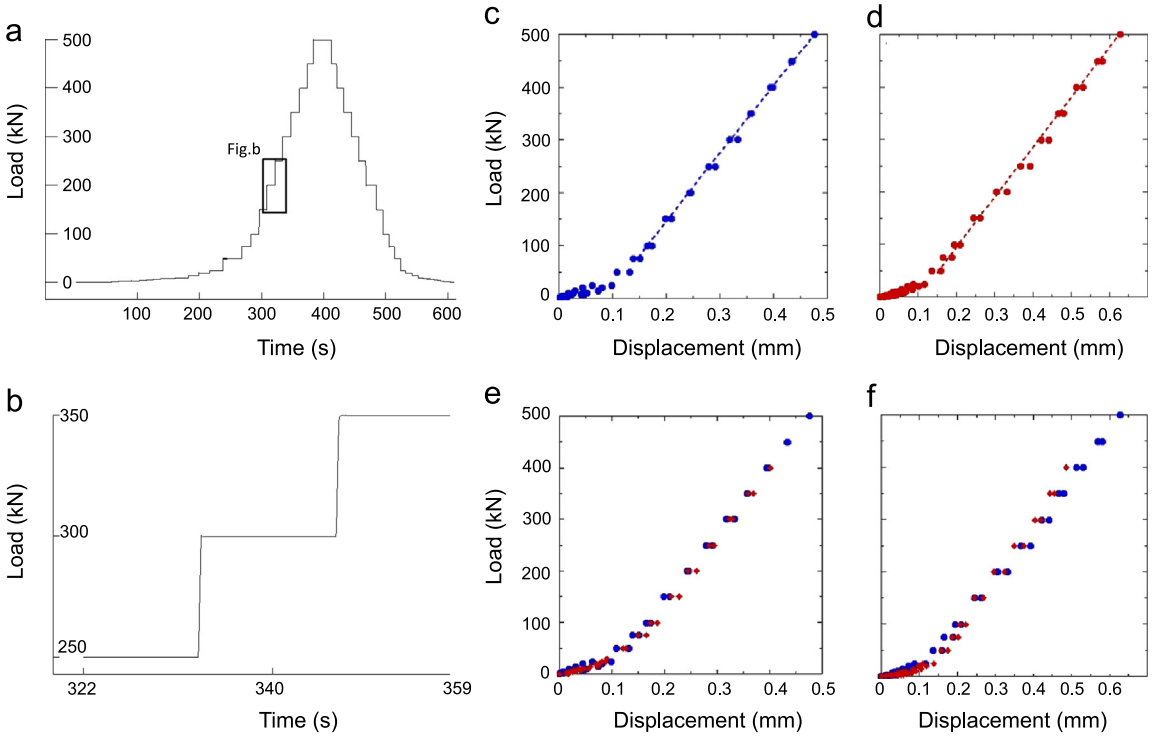

Fig. 8. Machine stiffness. (a) and (b) Experimental procedure adopted to evaluate the stiffness. (c) Horizontal and (d) vertical stiffness. (e) Horizontal and (f) vertical stiffness measured contemporaneously red points (see text for details) and comparison with horizontal stiffness only (blue points in (e)) and vertical stiffness only (blue points in (f)). (For interpretation of the references to colour in this figure legend, the reader is referred to the web version of this article.)

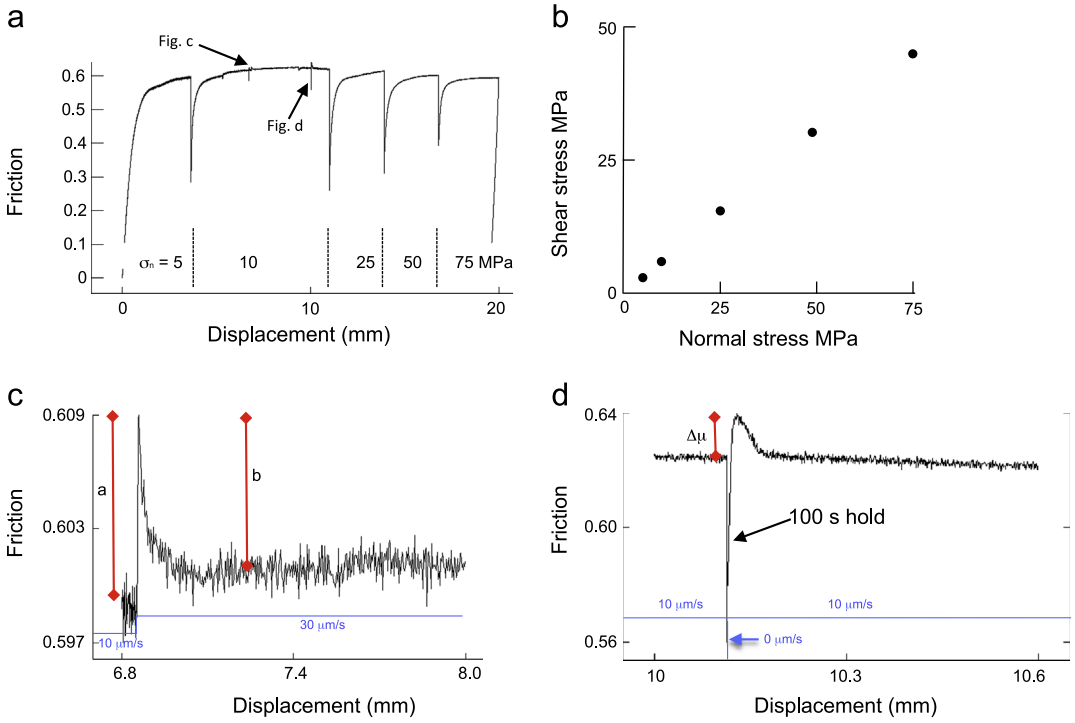

Fig. 9. Double direct experiments. (a) Displacement versus friction test results for granite. (b) Steady-state shear strength, measured during frictional sliding, plotted as a function of normal stress: data plot along a line with a slope of 0.6. (c) Velocity step with direct effect, *a*, and evolution effect, *b*. (d) Slide-hold-slide with re-strengthening, Dm.

Please cite this article as: Collettini C, et al. A novel and versatile apparatus for brittle rock deformation. Int J Rock Mech Mining Sci (2014), http://dx.doi.org/10.1016/j.ijrmms.2013.12.005

displacement versus load diagram (Fig. 8 c and d) both step-up and step-down measurements plot along the same line that defines a stiffness for the horizontal load frame of 1.283 kN/μm and for the vertical load frame of 0.928 kN/μm. At low stresses (<50 kN) the horizontal and vertical stiffness are lower. We also measured horizontal and vertical stiffness contemporaneously. We increased force on the horizontal piston and then we increased vertical force to the same amount. We adopted this procedure up to 500 kN of both vertical and horizontal forces and then we step-down similarly the two forces. Horizontal and vertical stiffness measured contemporaneously (Fig. 8e and f red points) are the same of those measured during loading the horizontal and vertical piston separately (Fig. 8e and f blue points), implying that the contemporaneous activity of the two piston does not alter the stiffness of the machine.

3.2. Frictional properties of granite and talc

We used two reference materials, granite and talc, to test if friction measurements performed with the new machine are reliable. Experiments were run in the double-direct shear configuration (biaxial configuration). Two identical layers of granular material, with dimensions of 5×5 cm^2 and thickness of 0.5 cm, were sandwiched between three steel forcing blocks (e.g. Fig. 1 and Section 2.5 for forcing block details). Experiments were conducted at room temperature and humidity. We determined steady-state friction values by shearing each sample at 10 μm/s for ~3 mm at normal stresses of 5, 10, 25, 50 and 75 MPa (Figs. 9 and 10a). At 10 MPa normal stress, we also conducted a single velocity step 10–30 μm/s (Fig. 9c), and slide-hold-slide with holding time of 100 s (Fig. 9d) to evaluate the frictional constitutive

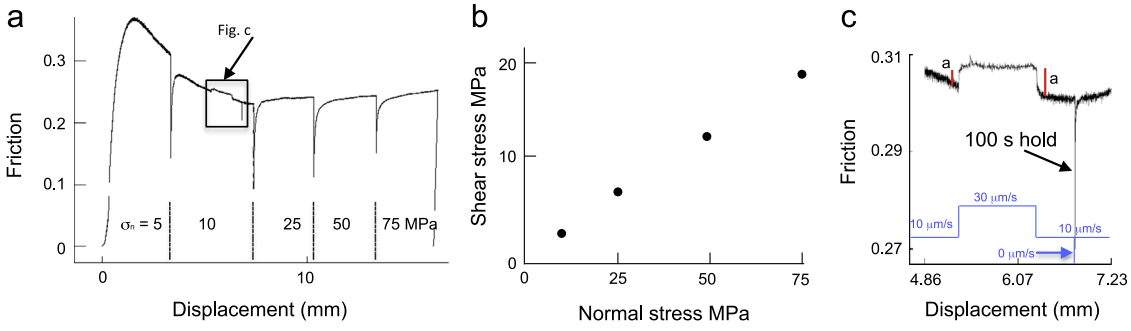

Fig. 10. Double direct experiments. (a) Displacement versus friction test results for talc. (b) Steady-state shear strength, measured during frictional sliding, plotted as a function of normal stress: data plot along a line with a slope of 0.25. (c) Two velocity steps with direct effect, *a*, and no evolution effect. Slide-hold-slide with no re-strengthening.

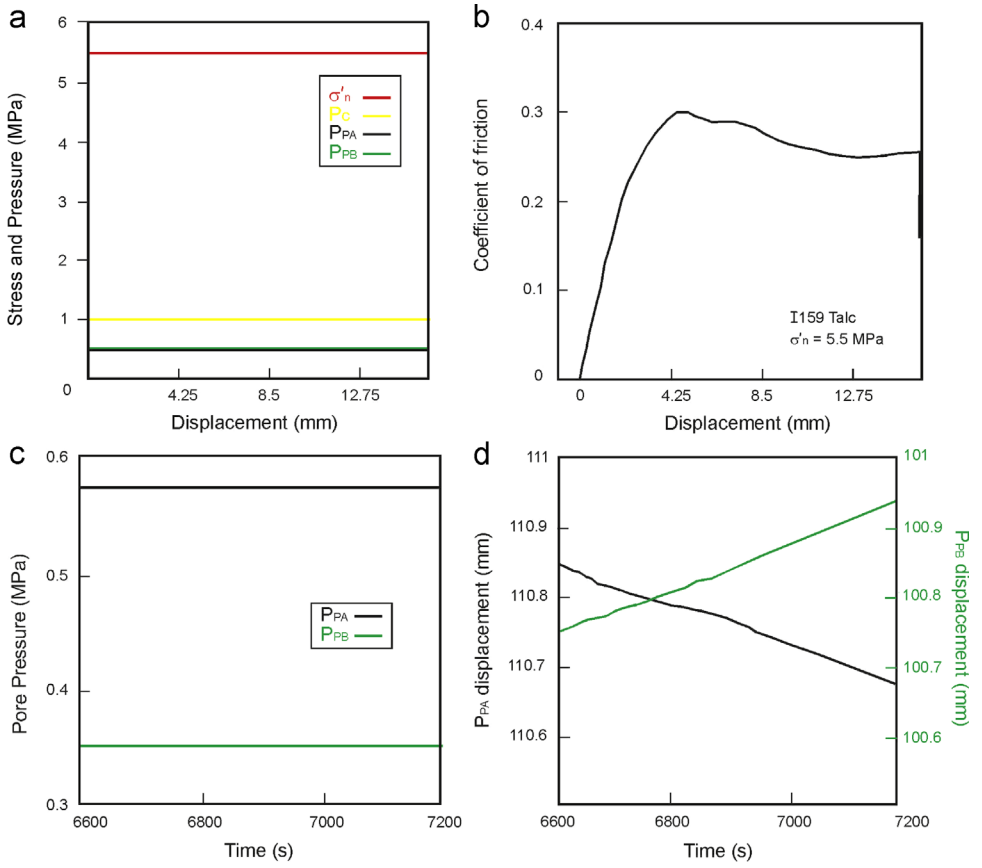

Fig. 11. Tests with pressure vessel.

Please cite this article as: Collettini C, et al. A novel and versatile apparatus for brittle rock deformation. Int J Rock Mech Mining Sci (2014), http://dx.doi.org/10.1016/j.ijrmms.2013.12.005

properties of each material. Velocity-stepping tests are used to evaluate frictional stability whereas slide-hold-slide tests are used to evaluate frictional healing.

For the different values of applied normal stress, the granite shows an initial stage of shear strengthening followed by a steady state friction coefficient that is constant for the different normal stresses (Fig. 9a). Data representing normal stress versus steady-state shear strength, measured during frictional sliding, are distributed along a line in agreement with a brittle failure envelope (Fig. 9b). The friction coefficient of granite, i.e. the slope of the straight line, is 0.6 in agreement with published data on granite [18].

The velocity dependence of friction is relevant to infer the seismic behaviour of brittle faults. For an e-fold change in sliding velocity from V_0 to V (with $V_0 < V$), if friction increases with increasing sliding velocity, this indicates a velocity strengthening behaviour that results in stable fault sliding and is associated with a seismic fault creep; if friction decreases, this indicates a velocity-weakening behaviour that is a prerequisite for unstable, stick–slip behaviour associated with earthquake nucleation [3,19,20]. During a velocity step, the instantaneous change in friction coefficient is defined as the direct effect, a; the decay to a new steady state is the evolution effect, b (Fig. 9c). The velocity step for the granite sample (Fig. 9c) shows an abrupt change in friction ($a=0.0071$) and a well-pronounced evolution effect ($b=0.0057$). The resulting positive a–b value is typical of powdered material at low shear strains (e.g. 3,20).

Slide-hold-slide tests are used to evaluate fault re-strengthening following a period of hold during which the sliding velocity is maintained at zero and the normal stress is constant [3]. Following a hold period of 100 s, the granite powder shows an increase in friction immediately upon re-shearing, then friction returns to the pre-hold steady-state value (Fig. 9d). The frictional healing, $\Delta_\mu=0.01$, is typical of strong powdered material [3,17].

For talc at low shear displacement, we did not reach a steady state condition. After an initial stage of shear strengthening, we observed strain weakening behaviour (Fig. 10a). A steady state in shear stress is obtained after shearing the sample for more than 5 mm. In a diagram of normal stress versus steady-state shear stress, measured during frictional sliding, data are distributed along a line in agreement with a brittle failure envelope (Fig. 10b). The friction coefficient of talc is 0.25 and it is consistent with published data [21–23]. The evolution of friction upon an instantaneous change in sliding velocity shows a well-pronounced direct effect (a in Fig. 10c) and no evolution effect. This is consistent with the behaviour of phyllosilicates [17,21,22,24]. Re-shearing after a hold period results in no re-strengthening (Fig. 10c), a typical behaviour of phyllosilicates e.g. [17,23].

3.3. Tests with pressure vessel

The first tests with the pressure inside the vessel have been performed in the double direct shear configuration using the forcing blocks and the jacketing system illustrated in Fig. 6. Here we present a test where we sheared two talc layers for 15 mm sheared at the constant boundary conditions: effective normal stress, $\sigma'_n=5.5$ MPa, confining pressure, $P_c=1$ MPa, and a pore pressure of 0.5 MPa. Although this test has been run at very low pressures in comparison to the capabilities of the BRAVA apparatus, the constant values measured while shearing (Fig. 11a) testify the accurate control that we can exert on these parameters. During the shear of the two talc layers (Fig. 11b), we observe an initial shear strengthening with a peak in friction of $\mu=0.3$, then a rollover and a steady state friction of 0.25. This value is consistent with the measurements at higher normal stress and at dry conditions (Fig. 10a). After shearing for 15 mm, we have stopped the vertical piston and then we have imposed a pore pressure gradient from P_{PA} to P_{PB} of 0.2 MPa (Fig. 11c). This resulted in a near constant velocity of movement of the two pore pressure intensifiers (Fig. 11d) that results in a nearly constant average flow rate for the system.

4. Future machine development

We are currently finalizing the designs of forcing blocks that will allow us to run experiments on cylindrical samples with diameters ranging from some centimeters to more than one decimeter. Using these forcing blocks, we will be able to conduct standard triaxial tests [18,25], measure porosity, permeability and elastic moduli during loading/unloading stress cycles [26–29] on large samples, ≈ 10 cm of diameter. With the new 20×20 cm^2 forcing blocks described here, we will also measure fault permeability during shearing, and loading/unloading stress cycles. Furthermore, the acoustic sensors will allow for the monitoring of different type of seismic signals emitted from our experimental fault as the result of variation in rock-type, sliding velocity, and confining and fluid pressure. In this way we aim to shed light on the processes at the base of the different types of seismic signals recently documented in seismically active regions [30–32].

Acknowledgments

This research has been carried out within the ERC Starting Grant GLASS no. (259256).

References

[1] Dieterich JH. Time-dependent friction in rocks. J Geophys Res 1972;77(20):3690–7.
[2] Mogi K, Mochizuki H. Measuring precursory strain prior to sudden slips along a heterogeneous artificial fault using a new double-shear type loading machine. In: Proc. Int. Symp. Earthquake Source Physics and Earthquake Precursors, 1992; pp. 43–47.
[3] Marone C. Laboratory-derived friction laws and their application to seismic faulting. Ann Rev Earth Planet Sci 1998;26:643–96.
[4] Dieterich JH. Potential for geophysical experiments in large-scale tests. Geophys Res Lett 1981;8:653–6.
[5] Rubinstein JL, Ellsworth WL, Beeler NM, Kilgore BD, Lockner DA, Savage HM. Fixed recurrence and slip models better predict earthquake behaviour than the time- and slip-predictable models: 2. Laboratory earthquakes. J Geophys Res 2012;117:B02307.
[6] Scholz C, Molnar P, Johnson T. Detailed studies of frictional sliding of granite and implications for the earthquake mechanism. J Geophys Res 1972;77(32):6392–406.
[7] Sone H, Hirose T, Uehara S, Noda H, Aizawa Y, Mizoguchi K, et al. Rock deformation apparatuses at Kyoto University. Jap J Struct Geol 2006;49:v–viii.
[8] Miao AL, Ma SL, Zhou YS. Experimental study on frictional stability transition and micro-fracturing characteristics for anhydrite fault zones. Chin J Geophys 2010;53(11):2671–80.
[9] Mair K, Frye KM, Marone C. Influence of grain characteristics on the friction of granular shear zones. J Geophys Res 2002;107(B10):2219.
[10] Anthony JL, Marone C. Influence of particle characteristics on granular friction. J Geophys Res 2005;110:B08409.
[11] Savage HM, Marone C. Effects of shear velocity oscillations on stick-slip behaviour in laboratory experiments. J Geophys Res 2007;112:B02301.
[12] Knuth MW, Tobin HJ, Marone C. Ultrasonic velocity of sheared granular material: implications for the evolution of dynamic elastic moduli with shear strain. Granular Matter 2013;15:499–515.
[13] Ikari M, Saffer DM, Marone C. Frictional and hydrologic properties of clay-rich fault gouge. J Geophys Res 2009;114:B05409.
[14] Samuelson J, Elsworth D, Marone C. Shear-induced dilatancy of fluid-saturated faults: experiment and theory. J Geophys Res 2009;114:B12404.
[15] Collettini C, Niemeijer A, Viti C, Marone CJ. Fault zone fabric and fault weakness. Nature 2009;462:907–10.
[16] Collettini C, Niemeijer A, Viti C, Smith SAF, Marone CJ. Fault structure, frictional properties and mixed-mode fault slip behaviour. Earth Planet Sci Lett 2011;311:316–27.
[17] Tesei T, Collettini C, Carpenter BM, Viti C, Marone C. Frictional strength and healing behaviour of phyllosilicate-rich faults. J Geophys Res 2012;117:B09402.
[18] Paterson MS, Wong TF. Experimental rock deformation: the brittle field. Berlin: Springer; 2005.

Please cite this article as: Collettini C, et al. A novel and versatile apparatus for brittle rock deformation. Int J Rock Mech Mining Sci (2014), http://dx.doi.org/10.1016/j.ijrmms.2013.12.005

[19] Dieterich JH, Kilgore B. Direct observation of frictional contacts: new insights for state dependent properties. Pure Appl Geophys 1994;143:283–302.
[20] Scholz CH. Earthquakes and friction laws. Nature 1998;391:37–42.
[21] Moore DE, Lockner DA. Talc friction in the temperature range 25°–400 °C: relevance for fault-zone weakening. Tectonophysics 2008;449:120–32.
[22] Ikari M, Marone C, Saffer DM. On the relation between fault strength and frictional stability. Geology 2011;39:83–6.
[23] Carpenter BM, Marone C, Saffer DM. Frictional behaviour of materials in the 3D SAFOD volume. Geophys Res Lett 2009;36:L05302.
[24] Niemeijer AR, Marone C, Elsworth D. Fabric induced weakness of tectonic faults. Geophys Res Lett 2010;37:L03304.
[25] Griggs DT, Turner FJ, Heard HC. Deformation of rocks at 500 °C to 800 °C. Rock Deformation (Geol. Soc. Am. Mem. 79). New York: Geological Society of America; 1960; 39–104.
[26] Faulkner DR, Mitchell TM, Healy D, Heap MJ. Slip on 'weak' faults by the rotation of regional stress in the fracture damage zone. Nature 2009;444:922–5.
[27] Heap MJ, Faulkner DR, Meredith PG, Vinciguerra S. Elastic moduli evolution and accompanying stress changes with increasing crack damage: implications for stress changes around fault zones and volcanoes during deformation. Geophys J Int 2010;183:225–36.
[28] Grindrod PM, Heap MJ, Fortes AD, Meredith PG, Wood IG, Trippetta F, et al. Experimental investigation of the mechanical properties of synthetic magnesium sulfate hydrates: implications for the strength of hydrated deposits on Mars. J Geophys Res 2010;115:E06012.
[29] Trippetta F, Collettini C, Meredith PG, Vinciguerra S. Evolution of the elastic moduli of seismogenic Triassic Evaporites subjected to cyclic stressing. Tectonophysics 2013;592:67–79.
[30] Marone, C. The Spectrum of Fault Slip Behaviors. EarthScope workshop, Portland, Oregon, October 2010.
[31] Peng Z, Gomberg J. An integrated perspective of the continuum between earth quakes and slow-slip phenomena. Nat Geosci 2010;3:599–607.
[32] Rubinstein JL, Shelly DR, Ellsworth WL. Non-volcanic tremor: a window into the roots of fault zones. In: Cloetingh S, Negendank J, editors. New Frontiers in Integrated Solid Earth Sciences; 2010. p. 287–314.

Please cite this article as: Collettini C, et al. A novel and versatile apparatus for brittle rock deformation. Int J Rock Mech Mining Sci (2014), http://dx.doi.org/10.1016/j.ijrmms.2013.12.005